Heat and Mass Transfer 39 (2003) 701–707
DOI 10.1007/s00231-002-0355-2

Analytical solutions for hydromagnetic natural convection flow of a particulate suspension through a channel with heat generation or absorption effects

Mansour A. Al-Subaie, Ali J. Chamkha

Abstract A continuum model for two-phase (fluid/particle) flow induced by natural convection is developed and applied to the problem of steady natural convection hydromagnetic flow of a particulate suspension through an infinitely long channel in the presence of heat generation or absorption effects. The walls of the channel are maintained at constant but different temperatures. The developed model accounts for particle-phase viscous stresses. Boundary conditions borrowed from rarefied gas dynamics are employed for the particle-phase wall conditions. Various closed-form solutions for different special cases are obtained. A parametric study of some of the physical parameters involved in the problem are performed to illustrate the influence of these parameters on the flow and heat transfer aspects of the problem.

List of symbols

c	Fluid-phase specific heat at constant pressure
c_p	Particle-phase specific heat at constant pressure
g	Gravitational acceleration
Gr	Grashof number
h	Channel width
H	Dimensionless buoyancy parameter
k	Fluid-phase thermal conductivity
M	Hartmann number
N	Interphase momentum transfer coefficient
N_T	Interphase heat transfer coefficient
P	Fluid-phase hydrostatic pressure
Pr	Fluid-phase Prandtl number
Q	Heat generation/absorption coefficient
S	Dimensionless particle-phase wall slip coefficient
T	Fluid-phase temperature
T_p	Particle-phase temperature
u	Fluid-phase dimensionless velocity
u_p	Particle-phase dimensionless velocity
U	Fluid-phase velocity
U_p	Particle-phase velocity
x, y	Cartesian coordinates

Received: 17 October 2001
Published online: 27 May 2003

M. A. Al-Subaie
Training Center – HRD,
Aramco Gulf Operations Co. Ltd. (AGOC),
P.O. Box: 688, Khafji 31971, Kingdom of Saudi Arabia

A. J. Chamkha (✉)
Department of Mechanical Engineering,
Kuwait University, Safat, 13060 Kuwait
E-mail: chamkha@kuc01.kuniv.edu.kw

Greek symbols

α	Velocity inverse Stokes number
β	Viscosity ratio
γ	Specific heat ratio
ε	Temperature inverse Stokes number
η	Dimensionless y-coordinate
θ	Dimensionless fluid-phase temperature
κ	Particle loading
μ	Fluid-phase dynamic viscosity
μ_p	Particle-phase dynamic viscosity
ρ	Fluid-phase density
ρ_p	Particle-phase density
σ	Fluid-phase electrical conductivity
ϕ	Dimensionless heat generation/absorption coefficient
ω	Particle-phase wall slip coefficient

1 Introduction

Natural convection flow of a particulate suspension represents one of the most interesting and challenging areas of research in heat transfer. Such flows are found in a wide range of applications including processes in the chemical and food industries, solar collectors where a particulate suspension is used to enhance absorption of radiation, cooling of electronic equipments, cooling of nuclear reactors, and heating of buildings via storage walls (trombe walls). In general, all applications of single-phase flow are valid for two-phase particulate suspension flow because the nature of real life dictates the presence of contaminating particles in fluids. Actually, there has been considerable work done on natural convection flows within vertical parallel-plate channels for a single phase. For example, Elenbass (1942) gave a detailed study of thermal characteristics of cooling by natural convection in smooth parallel-walled vertical channels using air as the fluid. Bodoia and Osterle (1962) investigated the development of free convection in air between heated vertical parallel plates. Aung (1972) presented a closed-form solution for the fully developed flow for laminar free convection in a vertical parallel-walled channel but with asymmetric heating conditions. The walls were maintained either at uniform heat flux or uniform wall temperature. Akbari and Borgers (1979) studied free convective laminar heat transfer between two parallel plates, each at some effective uniform temperature. A more detailed reference list was given by Muhanna (1991) who investigated

numerically laminar natural convection flows in obstructed vertical channels.

On the other hand, very little work has been found on natural convection flow of a particle-fluid suspension over and through different geometries. Recently, Chamkha and Ramadan (1998) and Ramadan and Chamkha (1999) have reported some analytical and numerical results for natural convection flow of a two-phase particulate suspension over an infinite vertical plate. Also, Okada and Suzuki (1997) have considered buoyancy-induced flow of a two-phase suspension in an enclosure. However, to the best of the author's knowledge, there is no work has been done on the problem of natural convection flow of a particulate suspension in vertical channels. Thus, there is a definite need for investigation of such a problem. This fact along with the possible application of this problem represents the significance of the present work. Hence, the objective of this research work is to perform an analytical investigation of steady natural convection laminar flow of a particulate suspension through an infinitely-long vertical parallel-plate channel.

2 Governing equations

In order to investigate the characteristics of natural convection two-phase flow in vertical channels in the presence of a uniform transverse magnetic field, one must start from the basic equations. These are the continuity equation, linear momentum balance and the energy balance of both phases. The basic equations which account for the magnetic field effect, particle-phase viscous stresses and the possible presence of heat generation or absorption effects can be written in the following vector form (see Marble, 1970 and Drew 1983) as:

$$\partial_t \rho + \nabla \cdot (\rho \mathbf{V}) = 0 \tag{1}$$

$$\rho(\partial_t \mathbf{V} + \mathbf{V} \cdot \nabla \mathbf{V}) = -\nabla P + \nabla \cdot (\mu \nabla \mathbf{V}) - \rho_p N(\mathbf{V} - \mathbf{V_p}) + \rho \mathbf{g} + \sigma(\mathbf{V} \times \mathbf{B}) \times \mathbf{B} \tag{2}$$

$$\rho c(\partial_t T + \mathbf{V} \cdot \nabla T) = \nabla \cdot (k \nabla T) + \rho_p c_p N_T (T_p - T) \pm Q(T - T_o) \tag{3}$$

$$\partial_t \rho_p + \nabla \cdot (\rho_p \mathbf{V_p}) = 0 \tag{4}$$

$$\rho_p(\partial_t \mathbf{V_p} + \mathbf{V_p} \cdot \nabla \mathbf{V_p}) = \nabla \cdot (\mu_p \nabla \mathbf{V_p}) + \rho_p N(\mathbf{V} - \mathbf{V_p}) + \rho_p \mathbf{g} \tag{5}$$

$$\rho_p c_p(\partial_t T_p + \mathbf{V_p} \cdot \nabla T_p) = -\rho_p c_p N_t (T_p - T) \tag{6}$$

where all variables are defined in the List of Symbols section. It should be noted that in writing equations (1) through (6), the magnetic Reynolds number is assumed to be small so that the induced magnetic field is neglected. In addition, no electric field is assumed to exist and that all of the viscous dissipation, Joule heating and the Hall effect are neglected.

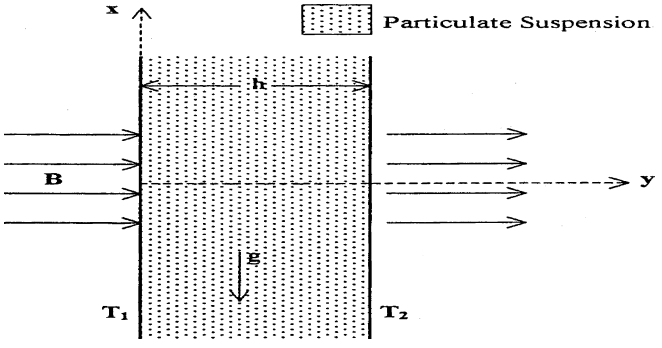

Fig. 1. Problem definition

This study considers steady, homogeneous with discrete particles, one dimensional, constant properties, incompressible, laminar, hydromagnetic natural convection fully developed two-phase (fluid-particle) flow in a parallel-plate channel. The channel walls are assumed to be infinitely long. This implies that the dependence of the variables on the x-direction will be negligible compared with that of the y-direction (see Fig. 1). Taking into account the above assumptions, equations (1) through (6) reduce to:

$$-\partial_x P + \mu \partial_{yy} U - \rho_p N(U - U_p) - \rho g - \sigma_o / \rho_o B^2 U = 0 \tag{7}$$

$$k \partial_{yy} T + \rho_p c_p N_T (T_p - T) \pm Q(T - T_o) = 0 \tag{8}$$

$$\mu_p \partial_{yy} U_p + \rho_p N(U - U_p) - \rho_p g = 0 \tag{9}$$

$$\rho_p c_p N_T (T_p - T) = 0 \tag{10}$$

It should be noted that the continuity equations of both phases are identically satisfied.

The pressure gradient can be eliminated from the linear momentum equation of the fluid phase by evaluating the governing equations at a reference point within the channel. Let "o" be a reference point within the channel such that $U = 0$, $T = T_o$, $\rho = \rho_o$, $\mu = \mu_o$, $\sigma = \sigma_o$, $U_p = U_{po}$, $T_p = T_{po}$, $\rho_p = \rho_{po}$ and $\mu_p = \mu_{po}$. Evaluating the governing equations at this reference point and employing the Boussinesq approximation gives:

$$\rho_{po}/\rho_o g + \mu_o/\rho_o \partial_{yy} U - \rho_{po}/\rho_o N(U - U_p) + \beta^* g(T - T_o) - \sigma_o/\rho_o B^2 U = 0 \tag{11}$$

where β^* is the volumetric expansion coefficient. The linear momentum equation of the fluid phase, equation (7), will now be replaced by equation (11) in the governing equations.

The physical boundary conditions for this problem are:

$$U(0) = U(h) = 0, \quad T(0) = T_1, \quad T(h) = T_2 \tag{12a–d}$$

$$U_p(0) = \omega \partial_y U_p(0) - g/N, \quad U_p(h) = -\omega \partial_y U_p(h) - g/N \tag{12e, f}$$

where h is the channel width, T_1 is the channel wall temperature at y = 0, T_2 is the channel wall temperature at y = h and ω is the particle-phase wall slip coefficient. Equations (12a) and (12b) indicate no slip conditions for the fluid phase at the walls of the channel.

Equations (12c) and (12d) suggest that the fluid temperatures at the walls of the channel are some constant values T_1 and T_2 such that $T_2 > T_1$. Equations (12e) and (12f) express proposed general wall boundary conditions for the particle phase at the channel walls borrowed from rarefied gas dynamics. It should be mentioned herein that the wall boundary conditions for the particulate phase are poorly understood at present. However, there is an experimental evidence that particles tend to slip at a boundary.

In order to solve this problem, it is convenient to non-dimensionalize the governing equations and conditions. This can be accomplished by using the following parameters:

$$\begin{aligned} &y = h\eta, \quad U = (\mu/\rho h)u, \quad U_p = (\mu/\rho h)u_p, \\ &T = (T_2 - T_o)\theta + T_o, \quad T_o = (T_1 + T_2)/2, \\ &T_p = (T_2 - T_o)\theta_p + T_o \end{aligned} \tag{13}$$

where η is the dimensionless coordinate, u and u_p are the dimensionless fluid- and particle-phase velocities, respectively, and θ and θ_p are the dimensionless fluid- and particle-phase temperatures, respectively. After performing the mathematical operations, the resulting dimensionless governing equations can be written as:

$$D^2u - \alpha\kappa(u - u_p) + Gr\,\theta + M^2u + \kappa H = 0 \tag{14}$$

$$(1/Pr)D^2\theta + \kappa\gamma\varepsilon(\theta_p - \theta) \pm \phi\theta = 0 \tag{15}$$

$$\beta D^2u_p + \alpha(u - u_p) - H = 0 \tag{16}$$

$$\varepsilon(\theta_p - \theta) = 0 \tag{17}$$

where D^2 denotes a second derivative operator with respect to η, $\alpha = h^2N\rho/\mu$, $\kappa = \rho_p/\rho$, $Gr = g\beta^*h^3\rho^2(T_2 - T_o)/\mu^2$, $M^2 = \sigma B^2h^2/\mu$, $H = gh^3\rho^2/\mu^2$, $\beta = \mu_p/(\kappa\mu)$, $Pr = \mu c/k$, $\gamma = c_p/c$, $\varepsilon = \rho N_T h^2/\mu$ and $\phi = Qh^2/(\mu c)$ are the momentum inverse Stokes number, particle loading, Grashof number, square of Hartmann number, buoyancy parameter, viscosity ratio, Prandtl number, specific heat ratio, temperature inverse Stokes number, and the heat generation or absorption parameter, respectively. The $\pm\phi$ stands for the problem with a heat generation coefficient (positive sign) and a heat absorption coefficient (negative sign).

The dimensionless boundary conditions become:

$$u(0) = u(1) = 0, \quad \theta(0) = -1, \quad \theta(1) = 1 \tag{18a–d}$$

$$\begin{aligned} &u_p(0) = SDu_p(0) - H/\alpha, \\ &u_p(1) = -SDu_p(1) - H/\alpha \end{aligned} \tag{18e, f}$$

where $S = \omega/h$ is the dimensionless particle-phase wall slip parameter. It should be mentioned that when $\beta = 0$ (inviscid particle phase), equations (18e, f) are ignored.

3 Results and discussion

Combining equations (15) and (17) and then solving for the fluid-phase temperature θ subject to the corresponding boundary conditions yields the following fully developed fluid-phase temperature profile:

$$\theta(\eta) = \left[\left(1 + \cos\sqrt{\phi\,Pr}\right)/\sin\sqrt{\phi\,Pr}\right] \times \sin\left(\sqrt{\phi\,Pr}\eta\right) - \cos\left(\sqrt{\phi\,Pr}\eta\right) \tag{19}$$

for a heat generating source and

$$\theta(\eta) = \sinh\left[0.5\sqrt{\phi\,Pr}(2\eta - 1)\right]/\sinh\left(0.5\sqrt{\phi\,Pr}\right) \tag{20}$$

for a heat absorbing sink.

Comparisons with previously published work for the case of a clear fluid (single phase) can be made. Assuming $\phi = 0$, then equations (19) and (20) reduces to:

$$\theta(\eta) = 2\eta - 1 \tag{21}$$

which is identical to that reported by Aung (1972). On the other hand, if the boundary condition of the fluid-phase dimensionless temperature was put equal to –1 at $\eta = -1$, instead of $\eta = 0$ in the present problem, then the predicted results are essentially identical to those reported by White (1991).

According to equation (17), the particle-phase temperature profile will be the same as that of the fluid-phase.

Equations (14) and (16) can be reduced to the following equations:

$$[D^4 - (\alpha/\beta + \kappa\alpha + M^2)D^2 - \alpha M^2/\beta]u = (\alpha/\beta - \phi\,Pr)Gr\,\theta(\eta) \tag{22}$$

$$[D^4 - (\alpha/\beta + \kappa\alpha + M^2)D^2 - \alpha M^2/\beta]u_p = (\alpha/\beta)Gr\,\theta(\eta) - HM^2/\beta \tag{23}$$

where $\theta(\eta)$ is given by equation (19) or (20) according to the sign of ϕ.

The above equations can be solved analytically to give the following general solutions:

$$u(\eta) = c_1e^{\zeta_1\eta} + c_2e^{-\zeta_1\eta} + c_3e^{\zeta_2\eta} + c_4e^{-\zeta_2\eta} + \chi_1\theta(\eta) \tag{24}$$

$$u_p(\eta) = d_1e^{\zeta_1\eta} + d_2e^{-\zeta_1\eta} + d_3e^{\zeta_2\eta} + d_4e^{-\zeta_2\eta} + \chi_2\theta(\eta) - H/\alpha \tag{25}$$

where

$$\zeta_1 = \sqrt{\left[\kappa\alpha + \alpha/\beta + M^2 + \sqrt{(\kappa\alpha + \alpha/\beta + M^2)^2 - 4\alpha M^2/\beta}\right]/2} \tag{26}$$

$$\zeta_2 = \sqrt{\left[\kappa\alpha + \alpha/\beta + M^2 - \sqrt{(\kappa\alpha + \alpha/\beta + M^2)^2 - 4\alpha M^2/\beta}\right]/2} \tag{27}$$

$$\chi_1 = (\alpha/\beta \pm \phi\,\mathrm{Pr})\mathrm{Gr}/[(\phi\,\mathrm{Pr})^2 \pm (\kappa\alpha + \alpha/\beta + \mathrm{M}^2)\phi\,\mathrm{Pr} + \alpha\mathrm{M}^2/\beta] \quad (28)$$

$$\chi_2 = (\alpha/\beta)\mathrm{Gr}/[(\phi\,\mathrm{Pr})^2 \pm (\kappa\alpha + \alpha/\beta + \mathrm{M}^2)\phi\,\mathrm{Pr} + \alpha\mathrm{M}^2/\beta] \quad (29)$$

The relationships which must exist among the constants c's and d's can be represented as:

$$\mathrm{c}_1 = (1 + \beta\zeta_1^2/\alpha)\mathrm{d}_1 \quad (30)$$

$$\mathrm{c}_2 = (1 + \beta\zeta_1^2/\alpha)\mathrm{d}_2 \quad (31)$$

$$\mathrm{c}_3 = (1 + \beta\zeta_2^2/\alpha)\mathrm{d}_3 \quad (32)$$

$$\mathrm{c}_4 = (1 + \beta\zeta_2^2/\alpha)\mathrm{d}_4 \quad (33)$$

Substituting the above relations back into equation (24) with the assumption that

$$\psi_1 = 1 + \beta\zeta_1^2/\alpha \quad (34)$$

$$\psi_2 = 1 + \beta\zeta_2^2/\alpha \quad (35)$$

gives the following general solution for the fluid-phase velocity

$$\mathrm{u}(\eta) = \psi_1\mathrm{d}_1\mathrm{e}^{\zeta_1\eta} + \psi_1\mathrm{d}_2\mathrm{e}^{-\zeta_1\eta} + \psi_2\mathrm{d}_3\mathrm{e}^{\zeta_2\eta} + \psi_2\mathrm{d}_4\mathrm{e}^{\zeta_2\eta} + \chi_1\theta(\eta) \quad (36)$$

The values of the constants d's can be determined by applying the velocities boundary conditions (18a, b, e, f) with their corresponding equations (25) and (36) to give

$$\psi_1\mathrm{d}_1 + \psi_1\mathrm{d}_2 + \psi_2\mathrm{d}_3 + \psi_2\mathrm{d}_4 = \chi_1 \quad (37)$$

$$\psi_1\mathrm{e}^{\zeta_1}\mathrm{d}_1 + \psi_1\mathrm{e}^{-\zeta_1}\mathrm{d}_2 + \psi_2\mathrm{e}^{\zeta_2}\mathrm{d}_3 + \psi_2\mathrm{e}^{-\zeta_2}\mathrm{d}_4 = -\chi_1 \quad (38)$$

For a heat generating fluid (source):

$$(1 - \mathrm{S}\zeta_1)\mathrm{d}_1 + (1 + \mathrm{S}\zeta_1)\mathrm{d}_2 + (1 - \mathrm{S}\zeta_2)\mathrm{d}_3 + (1 + \mathrm{S}\zeta_2)\mathrm{d}_4 = \chi_2\mathrm{S}\sqrt{\phi\,\mathrm{Pr}}\coth\left(0.5\sqrt{\phi\,\mathrm{Pr}}\right) + \chi_2 \quad (39)$$

$$(1 + \mathrm{S}\zeta_1)\mathrm{e}^{\zeta_1}\mathrm{d}_1 + (1 - \mathrm{S}\zeta_1)\mathrm{e}^{-\zeta_1}\mathrm{d}_2 + (1 + \mathrm{S}\zeta_2)\mathrm{e}^{\zeta_2}\mathrm{d}_3 + (1 - \mathrm{S}\zeta_2)\mathrm{e}^{-\zeta_2}\mathrm{d}_4 = -\chi_2\mathrm{S}\sqrt{\phi\,\mathrm{Pr}}\coth\left(0.5\sqrt{\phi\,\mathrm{Pr}}\right) - \chi_2 \quad (40)$$

For a heat absorbing fluid (sink):

$$(1 - \mathrm{S}\zeta_1)\mathrm{d}_1 + (1 + \mathrm{S}\zeta_1)\mathrm{d}_2 + (1 - \mathrm{S}\zeta_2)\mathrm{d}_3 + (1 + \mathrm{S}\zeta_2)\mathrm{d}_4 = \chi_2\mathrm{S}\sqrt{\phi\,\mathrm{Pr}}\left(1 + \cos\sqrt{\phi\,\mathrm{Pr}}\right)/\sin\sqrt{\phi\,\mathrm{Pr}} + \chi_2 \quad (41)$$

$$(1 + \mathrm{S}\zeta_1)\mathrm{e}^{\zeta_1}\mathrm{d}_1 + (1 - \mathrm{S}\zeta_1)\mathrm{e}^{-\zeta_1}\mathrm{d}_2 + (1 + \mathrm{S}\zeta_2)\mathrm{e}^{\zeta_2}\mathrm{d}_3 + (1 - \mathrm{S}\zeta_2)\mathrm{e}^{-\zeta_2}\mathrm{d}_4 = -\chi_2\mathrm{S}\sqrt{\phi\,\mathrm{Pr}}\left(1 + \cos\sqrt{\phi\,\mathrm{Pr}}\right)/\sin\sqrt{\phi\,\mathrm{Pr}} - \chi_2 \quad (42)$$

These equations, which will determine the d's, conclude the solution. However, this solution is valid for $0 \le \mathrm{S} < \infty$. Moreover, if $\mathrm{S} \to \infty$ (perfect particulate wall slip) then equations (39) and (40) will be replaced by

$$\zeta_1\mathrm{d}_1 - \zeta_1\mathrm{d}_2 + \zeta_2\mathrm{d}_3 - \zeta_2\mathrm{d}_4 = -\chi_2\sqrt{\phi\,\mathrm{Pr}}\coth\left(0.5\sqrt{\phi\,\mathrm{Pr}}\right) \quad (43)$$

$$\zeta_1\mathrm{e}^{\zeta_1}\mathrm{d}_1 - \zeta_1\mathrm{e}^{-\zeta_1}\mathrm{d}_2 + \zeta_2\mathrm{e}^{\zeta_2}\mathrm{d}_3 - \zeta_2\mathrm{e}^{-\zeta_2}\mathrm{d}_4 = -\chi_2\sqrt{\phi\,\mathrm{Pr}}\coth\left(0.5\sqrt{\phi\,\mathrm{Pr}}\right) \quad (44)$$

and equations (41) and (42) will be replaced by

$$\zeta_1\mathrm{d}_1 - \zeta_1\mathrm{d}_2 + \zeta_2\mathrm{d}_3 - \zeta_2\mathrm{d}_4 = -\chi_2\sqrt{\phi\,\mathrm{Pr}}\left(1 + \cos\sqrt{\phi\,\mathrm{Pr}}\right)/\sin\sqrt{\phi\,\mathrm{Pr}} \quad (45)$$

$$\zeta_1\mathrm{e}^{\zeta_1}\mathrm{d}_1 - \zeta_1\mathrm{e}^{-\zeta_1}\mathrm{d}_2 + \zeta_2\mathrm{e}^{\zeta_2}\mathrm{d}_3 - \zeta_2\mathrm{e}^{-\zeta_2}\mathrm{d}_4 = -\chi_2\sqrt{\phi\,\mathrm{Pr}}\left(1 + \cos\sqrt{\phi\,\mathrm{Pr}}\right)/\sin\sqrt{\phi\,\mathrm{Pr}} \quad (46)$$

The general solution given by equation (36) has the property that it reduces to that of the corresponding problem of natural convection two-phase flow with heat generation or absorption and in the absence of the magnetic field and the particle-phase viscous stresses. Thus, the fluid-phase velocity of such a problem is obtained by setting both β and M equal to zero and applying L'Hospital's rule to equations (36). If this is done, one obtains

$$\mathrm{u}(\eta) = \pm(\mathrm{Gr}/\phi\,\mathrm{Pr})[\theta(\eta) - 2\eta + 1] \quad (47)$$

where $\theta(\eta)$ is given by equation (19) or (20) according to the sign of ϕ. With this solution, the corresponding velocity profile for the particle phase is then obtained from equation (16) by setting β equals to zero to give

$$\mathrm{u_p}(\eta) = \mathrm{u}(\eta) - \mathrm{H}/\alpha \quad (48)$$

Figures 2 and 3 present typical velocity (u and $\mathrm{u_p}$) profiles for the fluid and particle phases for various values of the Hartmann number M, respectively. Application of a magnetic field normal to the flow direction creates a resistive force called the Lorentz force which acts in the direction opposite to the flow. This has the tendency to decrease the velocities of both phases. This is evident from Figures 2 and 3. In a buoyancy-driven flow as the one considered in the present work, an upward flow is induced in the immediate vicinity of the hot wall while a downward flow occurs close to the cold wall of the channel. This explains the reversed-flow phenomenon near the cold wall. It is clearly shown that as the strength of the magnetic field increases, the back flow close to the cold wall decreases. It should be noted that the particle-phase velocity is negative because the magnitude of the downward gravitational effect is greater than that of the induced upward flow effect for the parametric values employed to produce the results shown.

Some results for u, $\mathrm{u_p}$, θ and θ_p based on the closed-form solutions for the flow through a vertical channel in the presence of a heat generation (source) or a heat

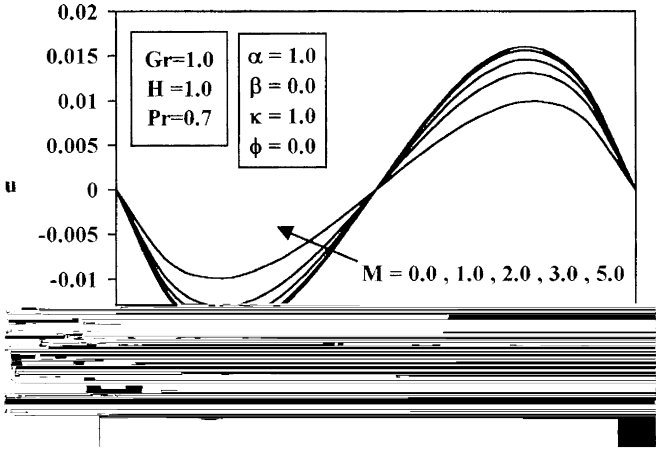

Fig. 2. Effects of M on Fluid-Phase Velocity Profiles

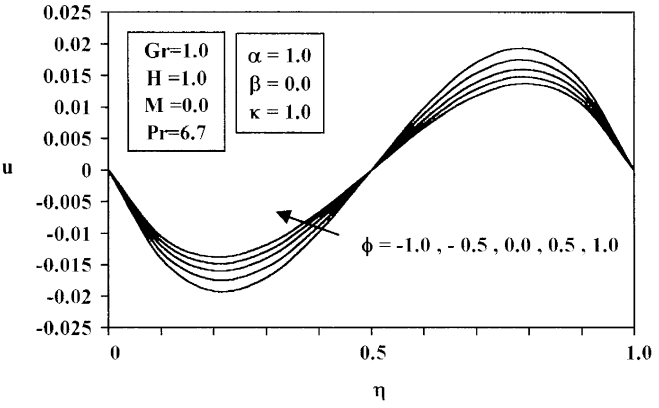

Fig. 4. Effects of ϕ on Fluid-Phase Velocity Profiles

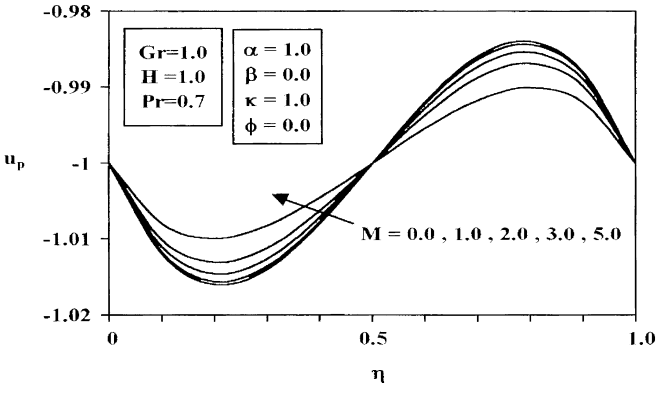

Fig. 3. Effects of M on Particle-Phase Velocity Profiles

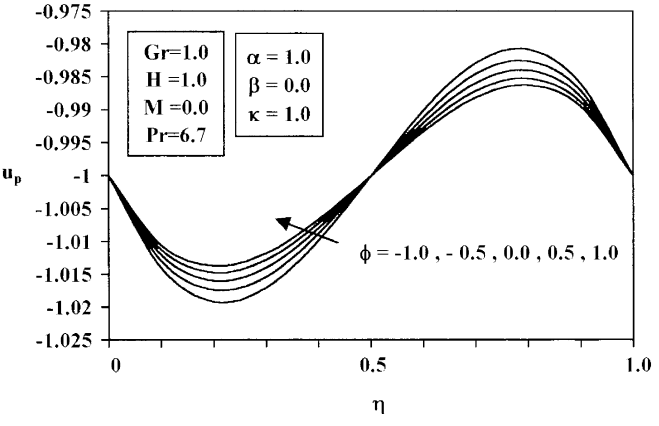

Fig. 5. Effects of ϕ on Particle-Phase Velocity Profiles

absorption (sink) term $\pm\phi\theta$ are presented in Figures 4 through 6. Figures 4 and 5 show representative velocity profiles for both phases (u and u_p) for different values of the heat generation or absorption coefficient ϕ. Increases in the values of ϕ decreases the fluid-phase temperature close to the hot wall of the channel. This has the tendency to decrease the buoyancy effects close to the hot wall. This produces a reduction in both the fluid- and particle-phase velocities there. The opposite behavior occurs close to the cold wall as clearly depicted in Figures 4 and 5. Figure 6 presents the temperature profiles for both the fluid and particle phases (θ and θ_p) for different values of ϕ. In the absence of heat generation or absorption effects ($\phi = 0$), the temperature profiles of both phases in the channel are linear. However, as ϕ increases (decreases), the temperature profiles become nonlinear and the temperature close to the cold wall increases (decreases), while the temperature close to the hot wall decreases (increases). This explains the behaviors in u and u_p discussed above.

The effects of varying the Prandtl number Pr on the temperature and velocity profiles of both phases are shown in Figures 7 through 9. Figure 7 shows this effect on the temperature profiles of both phases. In the absence of heat generation or absorption effects ($\phi = 0$), the temperature profiles of both phases in the channel are linear and independent of the Prandtl number Pr. However, in the presence of heat generation, $\phi = 1$ (heat absorption, $\phi = -1$) and as Pr increases, the temperature profiles become nonlinear and the temperature close to the hot wall decreases (increases) while the temperature close to the cold wall increases (decreases) in an asymmetrical fashion. The effects of Pr on the velocity profiles of the fluid and particle phases are shown in Figures 8 and 9, respectively. Increasing the value of Pr with $\phi = 1$ ($\phi = -1$) has the tendency to decrease (increase) the magnitude of both the fluid- and the particle-phase velocity profiles close to the hot wall, while the magnitude of the velocity profiles of both phases increase (decrease) close to the cold wall as Pr increases with $\phi = 1$ ($\phi = -1$). This behavior is consistent with the fact that as the fluid-phase temperature increases near a surface, the thermal buoyancy effect increases inducing higher flow rates of both phases there.

Figures 10 and 11 depict the effects of the ratio of the particle-to-fluid-phase viscosity β on the velocity profiles of both phases. Increases in the viscosity ratio β have the tendency to increase the magnitude of frictional effects for both phases in comparison with the buoyancy effects. This has the effect of decreasing the velocity of both phases as clearly depicted in Figures 10 and 11. In addition, Figure 11 shows that increases in the values of β have the tendency to flatten the particle-phase velocity profiles. Moreover, because the energy equations are uncoupled from the momentum equations, the temperature profiles

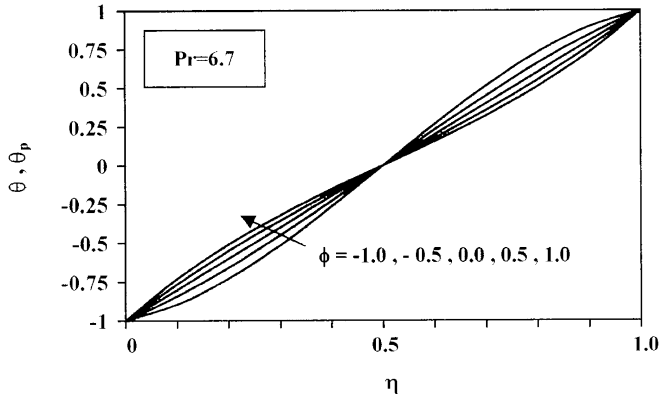

Fig. 6. Effects of ϕ on Fluid-Phase & Particle-Phase Temperature Profiles

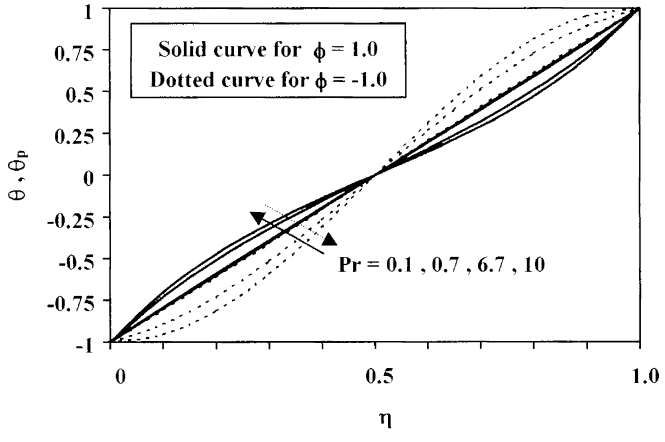

Fig. 7. Effects of Pr & ϕ on Particle-Phase Temperature Profiles

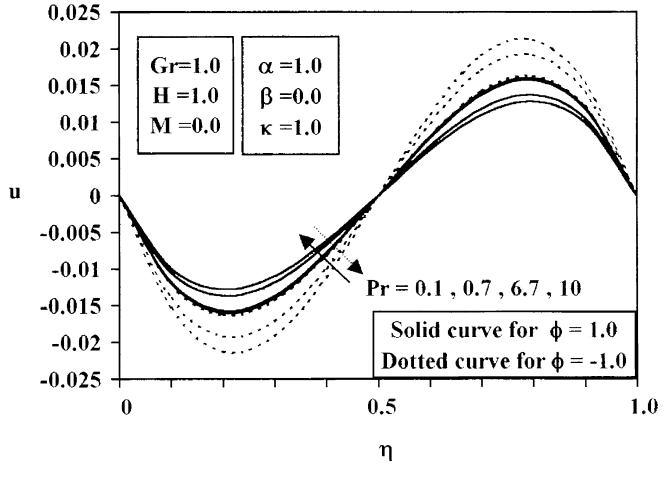

Fig. 8. Effects of Pr & ϕ on Fluid-Phase Velocity Profiles

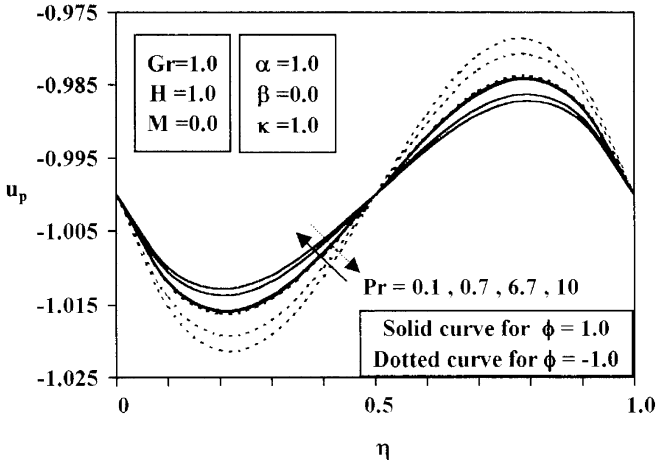

Fig. 9. Effects of Pr & ϕ on Particle-Phase Velocity Profiles

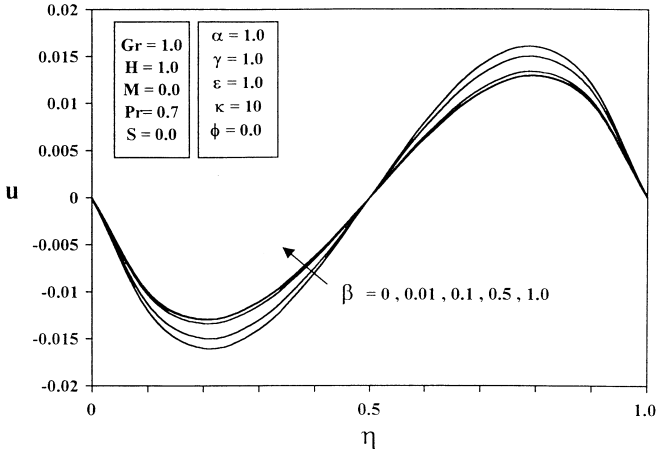

Fig. 10. Effects of β on Fluid-Phase Velocity Profiles

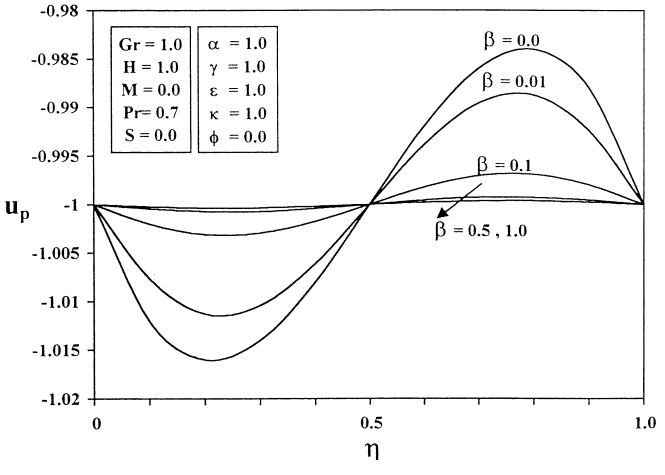

Fig. 11. Effects of β on Particle-Phase Velocity Profiles

for both phases are unaffected by the changes in the values of β.

Figure 12 illustrates the influence of the particle-phase slip coefficient S on the particle-phase velocity. In general, as the particle-phase wall slip increases from the limit of no particle-phase wall slip (S=0) to the limit of perfect particle-phase wall slip (S = ∞), it becomes easier for the carrier fluid to move it causing the particle-phase velocity to increase. In addition, the slip coefficient S seems to have no significant effect on the fluid-phase velocity and no effect on both fluid- and particle-phases temperature. The reasonable behavior exhibited in Figure 12 suggests that the use of the boundary conditions (18e,f) for the particle phase is adequate.

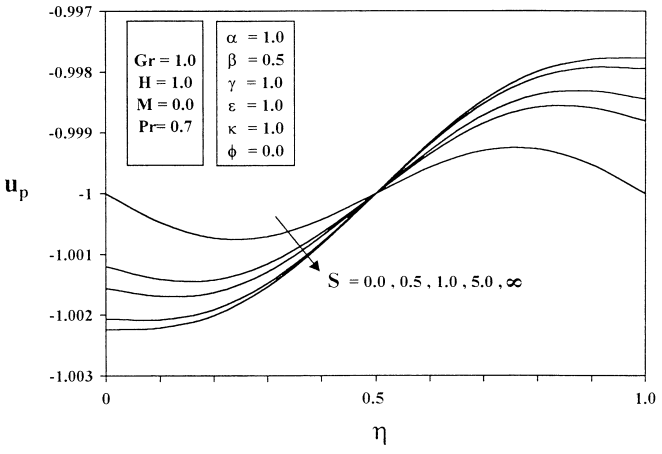

Fig. 12. Effects of S on Particle-Phase Velocity Profiles

4 Conclusions

The mathematical modeling of natural convection flow of a particulate suspension through a vertical parallel-plate channel in the presence of magnetic field and heat generation or absorption effects was formulated by applying the balance laws of mass, linear momentum, and energy for both the fluid and particle phases. The governing equations which account for particle-phase viscous effects were non-dimensionlized and solved analytically. Representative results were plotted to illustrate the influence of the physical parameters on the solutions. A reverse (back) fluid and particle flow situation near the cold wall was predicted and the velocity profiles had a symmetrical distribution. The magnetic field had the effect of reducing the velocity of the fluid phase which, in turn, reduced the particle-phase velocity. In the absence of viscous and magnetic dissipations, drag work, and heat generation or absorption, the temperature profiles of both phases were independent of the Prandtl number. Increases in the values of the heat generation (or absorption) coefficient caused the temperature close to the cold wall to increase (decrease) while the temperature close to the hot wall decreased (increased). Increases in the values of the heat generation (absorption) coefficient had a tendency to decrease (increase) the buoyancy effects close to the hot wall which produced reductions in the velocities of both phases close to the hot wall. The effect of the Prandtl number in the presence of heat generation (absorption) was found to decrease (increase) the temperature close to the hot wall, and to increase (decrease) the temperature close to the cold wall. Increases in the Prandtl number in the presence of heat generation (absorption) had a tendency to decrease (increase) the magnitudes of velocities of both phases close to the hot wall and to increase (decrease) them close to the cold wall. It is hoped that the results reported in this work will serve as a check for further theoretical modeling and a stimulus for experimental work on this problem.

References

Akbari HT; Borges R (1979) Finite Convective Laminary Flow Within Trombe Wall Channel, Solar Energy, Vol. 22, pp 165–174

Aung W (1972) Fully Developed Laminar Free Convection Between Vertical Plates Heated Asymmetrically. Int. J. Heat Mass Transfer, Vol. 15, pp 1577–1580

Aung W; Fletcher LS; Sernas V (1972) Development of Laminar Free Convection Between Vertical Flat Plates With Asymmetric Heating, Int. J. Heat Mass Transfer, Vol. 15, pp 2293–2328

Bodoia JR; Osterle JF (1962) The Development of Free Convection Between Heated Vertical Plates, ASME J. Heat Transfer, Vol. 84, pp 40–44

Chamkha AJ; Ramadan H (1998) Analytical Solutions for the Two-Phase Free Convection Flow of a Particulate Suspension Past an Infinite Vertical Plate, International Journal of Engineering Science, Vol. 36, pp 49–60

Drew DA (1983) Mathematical Modeling of Two-Phase Flow, Annual Review of Fluid Mechanics, Vol. 15, pp 261–291

Elenbass W (1942) Heat Dissipation of Parallel Plates By Free Convection, Physica, Vol. 9, pp 1–28

Marble FE (1970) Dynamics of Dusty Gases, Annual Review of Fluid Mechanics, Vol. 2, pp 397–447

Muhanna AM (1991) Numerical Investigation of Laminar Natural Convection Flows in Obstructed Vertical Channels, M. S. Thesis, King Fahd University of Petroleum and Minerals

Okada M; Suzuki T (1997) Natural convection of water-fine particle suspension in a rectangular cell, Int. J. Heat Mass Transfer, Vol. 40, pp 3201–3208

Ramadan H; Chamkha AJ (1999) Two Phase Free Convection Flow Over an Infinite Permeable Inclined Plate with Non-Uniform Particle-Phase Density, International Journal of Engineering Science, Vol. 37, pp 1351–1367

White F (1991) Viscous Fluid Flow, Second Edition, McGraw-Hill, New York